"High-Resolution, Ultra-Sensitive Magnetic Imaging Using an Ensemble of Nitrogen-Vacancy (NV) Centers in Diamond"

November 14, 2013

Sponsored by

Defense Advanced Research Projects Agency (DOD)
(Controlling DARPA Technical Office)

ARPA Order I642-00

Issued by U.S. Army Contracting Command – Redstone
Under
Contract No. W31P4Q-13-C-0064

Name of Contractor:	Quantum Diamond Technologies Inc.
Principal Investigator, Project Scientist, or Engineer:	Colin Connolly
Business Address:	4 Brattle Street, Suite 209, Cambridge, MA 02138
Phone Number:	(617) 320-4105

Effective Date of Contract:	November 30, 2012
Short Title of Work:	Option Final Technical Report
Contract Expiration Date:	December 31, 2013
Reporting Period:	August 28 – November 14, 2013

DISCLAIMER

Table of Contents

1. Introduction

Magnetic field imaging with nitrogen-vacancy (NV) centers in diamond has received great attention in recent years owing to a unique ability to combine high resolution, high sensitivity, and general-purpose suitability to a wide range of conditions. Other technologies generally cannot provide similar performance and speed at room temperature. For example, high-sensitivity techniques that employ superconducting quantum interference devices (SQUIDs) suffer from poor resolution (100-200 μm) limited by the sensor's need to be isolated at low temperature. Magnetic force microscopy (MFM) can provide very high resolution magnetic information, but scanning the sensor across each pixel takes hours even for fields of view no larger than a few microns. Imaging using arrays of sensors, such as those based on the Hall effect, are limited by sensor size and the challenge of uniquely addressing each sensor. For the case of Hall effect sensors, each sensor requires four electrical connections and significant current densities that present a formidable challenge for high-resolution imaging with thousands or millions of sensors.

In contrast, individual NV centers in diamond are extremely sensitive to magnetic fields [1, 2] and can be localized remotely under ambient conditions to within a few nanometers, limited only by the optical readout system. Very large ensembles of NV centers concentrated at the surface of a diamond chip constitute a magnetic imaging sensor: NV fluorescence collected with and without microwave excitation carries information about the local magnetic field observed by each NV center, and focusing the fluorescence onto a multi-megapixel camera creates a wide-field image with diffraction-limited resolution [3, 4]. All NV centers are interrogated in parallel such that the entire image can be obtained rapidly, with photon shot noise-limited magnetic sensitivity near 10 μT /sqrt(Hz) (for 1-μm^2 pixel size) [3].

With diamond wide-field magnetic imaging, applications previously limited by low resolution can obtain dramatically enhanced detail without sacrificing sensitivity. Conversely, high-resolution images can be obtained over millions of pixels simultaneously rather than laboriously scanning each pixel sequentially. The diamond sensor itself produces no net magnetic field and hence does not disturb high-sensitivity measurements, a potential side effect of technologies like MFM that employ magnetic materials close to the sample of interest. In addition, diamond is inert and biocompatible, allowing measurements to be made in solution and in direct sample contact without disturbance.

During this Phase I Option effort, Quantum Diamond Technologies, Inc., (QDTI) advanced the capabilities of wide-field magnetic imaging using diamond, including especially the application to rapid imaging of millimeter-scale fields of view (FOVs). Technical improvements during the Phase I Option are demonstrated through the Phase I target application, detection of magnetically-tagged rare cells

2. Technical development of wide-field magnetic imaging

Optical imaging system

Imaging wide fields of view (FOVs) at high resolution places increased demands on the optical system used for imaging NV center fluorescence. First, the magnification of the imaging system must be suitably low to match the FOV size to that of the camera CCD or CMOS sensor. For typical sensor sizes of ≈1 cm^2, a 1-mm^2 FOV is therefore limited to magnification of 10. To ensure no loss of sensitivity, the numerical aperture (NA) must remain high for the entire FOV. This in general implies that the imaging lenses must be larger.

The broad spectrum of NV center fluorescence (≈100 nm wide) requires correction of chromatic distortion, and high-resolution imaging with high NA further demands that other aberration be controlled, as well. As a result, commercial microscope objectives, which are designed to address these needs simultaneously, are an appropriate tool for imager development. This is especially true for a general-purpose magnetic imaging device that must excel by several metrics, although specific applications may allow for cost-savings through simpler components.

For detection of human tumor cells, typically ≈10 μm in size (see Fig. 4a), resolution may be sacrificed in order to achieve a wider FOV and correspondingly higher cell detection throughput. Therefore, in this case, aberration an order of magnitude greater than the diffraction limit can be tolerated without significant degradation of detection capability. This can allow imaging with simple achromatic doublet lenses. The highest NA is still achieved with more complex objectives, and so wide-field applications demanding the highest sensitivity or imaging speed cannot rely on a simple optical system.

Bias magnetic field homogeneity

Over a small FOV, it is straightforward to engineer a static magnetic bias field B_0 that is relatively homogeneous using only one or two small permanent magnets. Over a larger FOV, however, this task becomes more challenging. B_0 determines the optically detected magnetic resonance (ODMR) frequency, and hence inhomogeneity leads to broadening that can degrade magnetic imaging sensitivity. The challenge can be decomposed into two primary issues: (1) ensuring homogeneity of the projection of the bias magnetic field onto the NV axis; and (2) maintaining a constant angle between the bias magnetic field and NV axis throughout the FOV.

First we consider homogeneity of the projection of B_0 onto the NV axis. In a DC ODMR measurement, the maximum magnetic field sensitivity is obtained when ODMR measurements are made only at

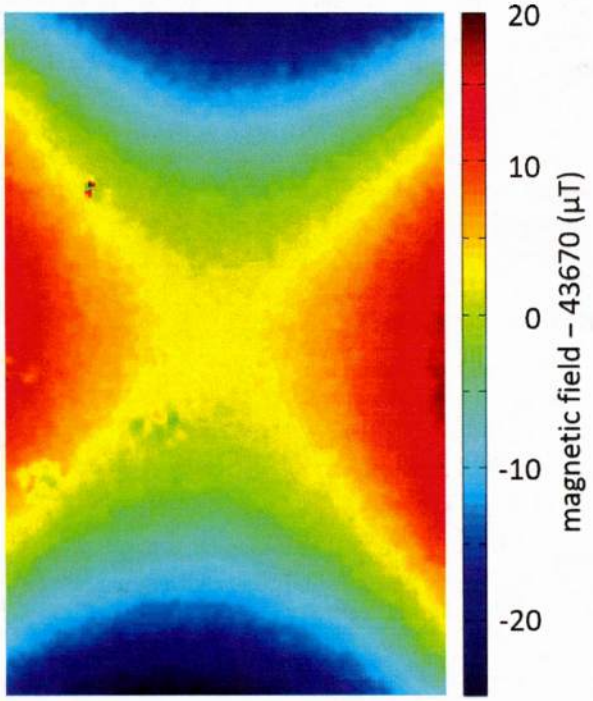

Figure 1: Inhomogeneity of B_0, the bias magnetic field magnitude, which is created using two permanent magnets spaced by approximately 4 cm in the horizontal direction (they are also separated in the dimension normal to the page). Along the separation axis, the vertical field gradients produced by the two magnets are zero and the horizontal gradients ($B_{0,1}$) are equal and opposite, cancelling to zero. What is left is a constant field of approximately 44 mT and a 1,000 times weaker curvature component ($B_{0,2}$). This inhomogeneity is removed from magnetic field images by fitting the image to a second-order polynomial in two-dimensions.

microwave frequencies located one half width half maximum (HWHM) from the resonance, where the NV fluorescence rate is maximally sensitive to changes in magnetic field. For a fixed microwave frequency, as B_0 varies the resonance shifts and the magnetic field sensitivity falls. Hence the required B_0 homogeneity to avoid degrading sensitivity is that which produces ODMR resonance shifts that are significantly less than the resonance line width. For line width of order 1 MHz and NV center gyromagnetic ratio of 2.8 MHz/G, this requires the homogeneity of B_0 to be less than ≈30 μT, or ≈0.1% of a 30 mT bias field.

Figure 1 shows an image obtained with a wide-field diamond magnetic imager. The bias field of approximately 40 mT is generated by two permanent magnets symmetrically spaced along a line parallel to the NV axis that passes through the center of the FOV. The magnetic field projection produced by each magnet along the NV axis can be expressed as a series expansion,

$$B_0(x) = B_{0,0} + B_{0,1}\, x + B_{0,2}\, x^2 + O(x^3)$$

where $B_{0,i}$ is the coefficient of the i^{th} order component of the field. If the two magnets have the same orientation and are placed equidistant from the diamond, then each contributes identical values of $B_{0,0}$ and $B_{0,2}$, but $B_{0,1}$ values of opposite sign that cancel. The result is a static magnetic field $B_0 = 2 \times B_{0,0}$ with curvature that worsens at the edges of the FOV (Fig. 1). A similar curvature of opposite sign is predicted in the dimension normal to the NV axis. The static field inhomogeneity is given by

$$\frac{\Delta B_0}{B_0} \approx \frac{B_{0,2} L^2}{4 B_{0,0}}$$

where L is the FOV size.

The curvature is reduced by increasing the transverse size of the magnets in comparison to their magnet spacing. As large permanent magnets produce large fields and forces nearby that may be problematic, an alternate approach would be to use an array of magnets or single shaped magnet to engineer a more homogeneous field. Mediating the curvature in B_0 will be necessary to exploit the full sensitivity of diamond magnetic imaging over wide fields of view.

The second issue concerning magnetic field homogeneity is the angle between B_0 and the NV axis. One process in particular is highly sensitive to this angle: optical polarization of the nitrogen (N) nuclear spin. It has been demonstrated that an energy level anti-crossing (LAC) near 50 mT in the NV center excited state allows for spin exchange between the NV electronic spin and the N nucleus, and hence transfer of polarization from the electronic spin to the nuclear spin [5, 6]. Such polarization has been observed in both ^{14}N and ^{15}N and at purities above 98%. Most relevant here, the polarization has also been observed to sensitively depend upon the alignment of the magnetic field and NV axes, with the greatest polarization found when the two are parallel [5].

The immediate effect of nuclear spin polarization is an asymmetry in the multi-peak ODMR resonance (Fig. 2), reflecting increased population in one nuclear spin state. If the nuclear spin is fully polarized, only one peak is visible, but others will be present for imperfect polarization. The degree of polarization is determined by the competition between the rate of optical pumping and that of nuclear spin relaxation caused by interactions with the environment. At higher optical intensity, greater polarization is observed, and over a broader range of magnetic fields near the excited state LAC [5].

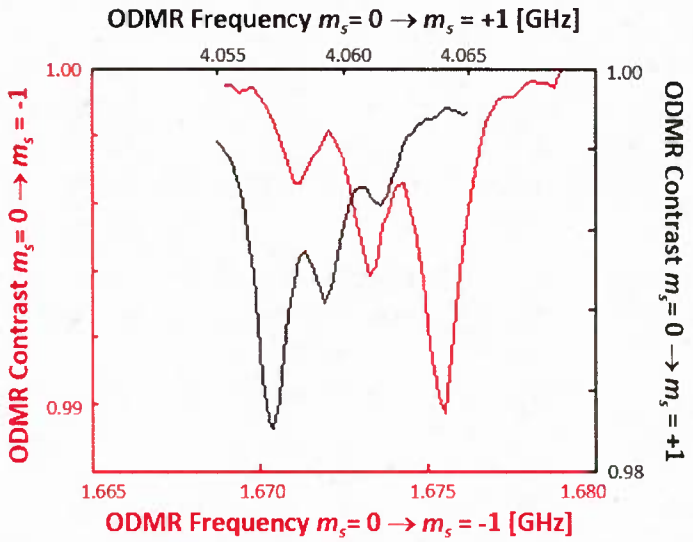

Figure 2: Optically detected magnetic resonance (ODMR) spectra for the m_s = 0 → ±1 resonances, integrated over a region of diamond with many NV centers at a magnetic field magnitude of 43 mT. The optical excitation power is approximately 300 mW over a 0.3-mm^2 spot. The asymmetry in the spectrum is due to polarization of the N nuclear spin induced by spin exchange with the NV electronic spin in the NV excited state. Faster and purer nuclear polarization occurs near the excited state level anti-crossing (LAC) near 50 mT, and for high optical intensity.

Nuclear polarization presents both opportunities and challenges for magnetic field imaging. On the one hand, a highly-polarized state increases contrast for the associated ODMR peak, increasing magnetic field sensitivity. On the other hand, instability or inhomogeneity of nuclear spin polarization can degrade or systematically bias the measurement. In particular, varying population in states other than the polarized state will both: (1) add noise to the measurement of the polarized ODMR resonance; and (2) shift the apparent center of the polarized resonance due to varying contributions of the sloped tails of nearby resonances. The latter effect is particularly pronounced when the resonance line width is comparable to or larger than the hyperfine splitting between peaks. Image artifacts can then arise due to these line shifts' dependence on the local optical power and on the local angle between the bias magnetic field B_0 and the NV axis.

Control of excitation beam variation

During the Phase I Base period, QDTI observed that instability of the 532-nm NV excitation beam could generate significant magnetic imaging artifacts [7]. In particular, motion of the beam with respect to the diamond sensor causes anti-correlated noise at regions of the FOV with opposite intensity gradient in the direction of motion. Such noise leads to magnetic field shifts correlated to the local intensity gradient, creating artifacts sensitive to the intensity profile.

Excitation beam motion was controlled in Phase I by the use of a single-mode optical fiber to fix the beam's spatial mode. This approach successfully reduced motion artifacts, however the fiber introduced power fluctuations to the output beam (e.g., fluctuations in fiber input coupling due to the same beam motion). While, power fluctuations could be partially compensated by monitoring the beam power with a beamsplitter and photodiode, the residual uncompensated intensity noise remained significant. Additionally, using a single-mode fiber reduces the maximum excitation beam intensity and introduces thermal sensitivity to intensity fluctuations, exacerbating their effect.

In the Phase II Option, the fiber was removed in favor of a much shorter beam path between the laser source and diamond sensor. In addition, a telescope with unity magnification was used to further collapse the beam path and suppress angular deviations. Including the telescope, the beam path was

approximately 30 cm, a distance that could be significantly reduced with further development. Since the laser source used for this work (Verdi G7, Coherent Inc., Santa Clara, CA) was quite stable in intensity (root-mean-squared (RMS) fluctuations ≈ 3×10^{-5} between successive 100-ms exposures), no photodiode intensity reference was necessary.

With the shorter beam path, motion-induced artifacts were greatly reduced, although not eliminated entirely. Images can be obtained within 1 minute of averaging with motion-induced RMS noise well below 1 μT, with the great majority of the noise occurring on length scales longer than 30 μm (Fig. 3). This performance allows for shot noise-limited detection of smaller objects such as cancer cells, as described below in Section 3.

3. Cell detection with wider field of view

The primary improvements made in the Phase I Option are those described in Section 2: use of a lower-magnification commercial objective; careful alignment of two permanent magnets for first-order cancellation of magnetic field inhomogeneity; and free-space excitation laser coupling over a short path length to reduce noise from beam motion and intensity fluctuations.

The diamond used for magnetic imaging in the Phase I Option is an electronic-grade single-crystal CVD chip (Element Six) implanted with ^{14}N at 14 keV and subsequently annealed to create a surface layer of NV centers at a depth of approximately 20 nm. The implanted area is nearly 4 mm^2, although defects in

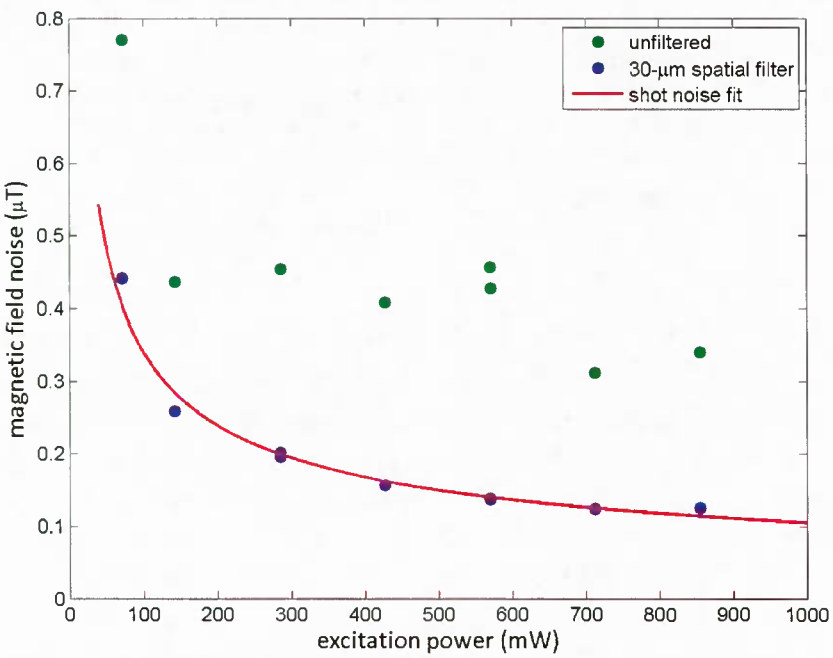

Figure 3: Magnetic imaging noise with increasing NV excitation power at 532 nm. Data points are root-mean-squared (RMS) noise measured over a field of view (FOV) approximately 0.3 mm^2 in size. When spatially filtered to remove large-scale structure (high pass filter with 30 μm wavelength cutoff), the noise is inversely proportional to the square root of the excitation power, as expected for shot noise-limited imaging. The additional noise on larger scales is attributed to image artifacts caused by beam motion and inhomogeneous excitation intensity.

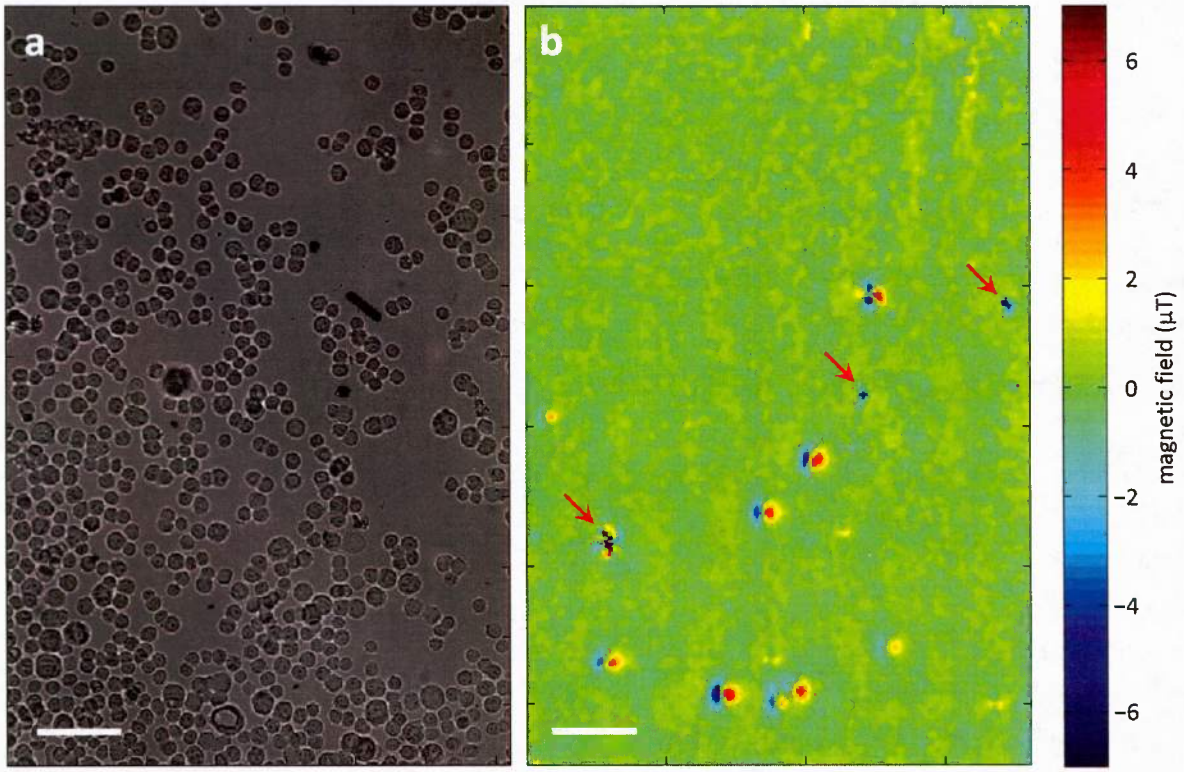

Figure 4: (a) Optical transmission and (b) magnetic images of the same field of view (FOV) filled with over 700 cells from the SK-BR-3 cancer cell line. Approximately 1% of the cells were labeled with magnetic nanoparticles (MNPs) before being mixed into identical unlabeled candidates. The magnetic image shows magnetic signals corresponding to several cells, in agreement with the 1% mixing fraction. Red arrows indicate locations of defects in the diamond sensor (e.g., gaps in the implanted NV layer). The magnetic image has been high-pass filtered with an 80-μm wavelength cutoff to remove large-scale artifacts caused by excitation beam motion. This process does not significantly reduce the sensitivity to cell-scale magnetic structure. Scale bars are 100 μm.

the implantation produced a number of gaps in the NV layer over which magnetic imaging is not possible.

Figure 4 gives an example image of a FOV filled with over 700 cells from the SK-BR-3 cancer cell line. A fraction of the cells were first magnetically labeled with 20-nm iron oxide nanoparticles conjugated to antibodies targeting the surface marker Her2. These labeled cells were then mixed as a 1% fraction into a population of unlabeled cells before introducing the mixture to the diamond surface. The magnetic image from the diamond shows a clear signature from several of the cells, in good agreement with the 1% labeling fraction.

The FOV size in Fig. 4 is approximately 600 μm × 950 μm ≈ 0.6 mm^2. In this case, the FOV size is defined by the excitation laser beam spot. The beam spot size can be expanded to increase the FOV area at the cost of a proportional reduction in NV fluorescence rate and hence a proportional increase in imaging time for the same image quality. The optical system used here is capable of imaging triple this FOV area, limited instead by the size of the CMOS sensor in the camera. Approximately another factor of two in FOV area can be obtained by reducing the magnification to fit the image onto the camera sensor. Only

at this point would the FOV be limited by the optical imaging system, in particular the back aperture of the microscope objective. It is therefore straightforward to extend this imaging to a FOV of several mm^2 without major modification. Significant additional FOV area approaching 1 cm^2 can be obtained with a lower-magnification objective and larger diamond sensor, with some loss of imaging resolution due to finite pixel size.

4. Summary

During the Phase I Option, QDTI made significant progress in expanding the FOV available for magnetic imaging of magnetically-labeled human cancer cells. This effort, and the demonstration here of detecting 1% target cells among 10^3 candidate cells, charts a path forward to achieving highly parallel detection of rare cells from larger candidate pools (10^5 to 10^6 cells) imaged simultaneously. This would enable this technology to compete with fluorescence detection methods for high-throughput scanning of patient blood samples.

Furthermore, the technical progress achieved here will inform additional magnetic imaging applications for which it is critical to achieve wide FOV with high resolution, such as measurement of magnetic microstructure in solid materials rapidly and simultaneously over a range of length scales.

5. References

[1] J. Taylor, P. Cappellaro, L. Childress, L. Jiang, D. Budker, P. Hemmer, A. Yacoby, R. Walsworth and M. Lukin, "High-sensitivity diamond magnetometer with nanoscale resolution," *Nature Physics,* vol. 4, no. 10, pp. 810-816, 2008.

[2] J. Maze, P. Stanwix, J. Hodges, S. Hong, J. Taylor, P. Cappellaro, L. Jiang, M. G. Dutt, E. Togan, A. Zibrov and others, "Nanoscale magnetic sensing with an individual electronic spin in diamond," *Nature,* vol. 455, no. 7213, pp. 644-647, 2008.

[3] M. L. Pham, D. Le Sage, P. L. Stanwix, T. K. Yeung, D. Glenn, A. Trifonov, P. Cappellaro, P. R. Hemmer, M. D. Lukin, H. Park, A. Yacoby and R. L. Walsworth, "Magnetic field imaging with nitrogen-vacancy ensembles," *New Journal of Physics,* vol. 13, no. 4, p. 045021, 2011.

[4] B. Maertz, A. Wijnheijmer, G. Fuchs, M. Nowakowski and D. Awschalom, "Vector magnetic field microscopy using nitrogen vacancy centers in diamond," *Applied Physics Letters,* vol. 96, no. 9, pp. 92504-92504, 2010.

[5] V. Jacques, P. Neumann, J. Beck, M. Markham, D. Twitchen, J. Meijer, F. Kaiser, G. Balasubramanian, F. Jelezko and J. Wrachtrup, "Dynamic polarization of single nuclear spins by optical pumping of nitrogen-vacancy color centers in diamond at room temperature," *Physical Review Letters,* vol. 102, no. 5, p. 057403, 2009.

[6] R. Fischer, A. Jarmola, P. Kehayias and D. Budker, "Optical polarization of nuclear ensembles in diamond," *Physical Review B,* vol. 87, no. 12, p. 125207, 2013.

[7] Quantum Diamond Technologies, Inc., "High-Resolution, Ultra-Sensitive Magnetic Imaging Using an Ensemble of Nitrogen-Vacancy (NV) Centers in Diamond," July Contract No. W31P4Q-13-C-0064, Phase I Final Report, July 26, 2013.

6. Publications this period

There were no publications sponsored by this contract in this reporting period.